Determination of generalized fracture toughness in composite multimaterial closed corners with two singular terms. Part II: experimental results.

D. Vicentini, A. Barroso, J. Justo, V. Mantič, F.París.

Group of Elasticity and Strength of Materials, School of Engineering, University of Seville, Camino de los Descubrimientos s/n, 41092 Seville, Spain.

Abstract: In this paper the experimental part of the Generalized-Fracture-Toughness determination in multimaterial closed corners with two stress singularities is presented. The so-called Generalized-Fracture-Toughness (the critical values of the generalized stress intensity factors (GSIF) at failure) can only be determined if each singular term can be isolated, after which the value of GSIF at the instant of failure can be evaluated. The loading configuration which allows the isolation of any of the stress singularities was analyzed in Part I, while the details of the testing procedure and postprocessing of the experimental results are covered in the present paper. The proposed test is a novel modified configuration of the Brazilian test in which the multimaterial corner tip is located at the centre of the disk. A failure envelope based on the GSIFs and Generalized-Fracture-Toughness values at the corner tip is defined and proposed as a failure criterion for joints of this type. Results for real adhesively bonded double-lap joints are presented showing a satisfactory agreement with the proposed failure criterion.

Keywords: Generalized-Fracture-Toughness, Brazilian test, bimaterial corner, stress singularities, composites, adhesive joints.

1. Introduction

The experimental determination of a fracture toughness value of a crack is typically based on the evaluation of the experimental failure load (obtained by means of a specific test configuration) in the known explicit expression of the asymptotic stress field controlled by a single stress intensity factor (SIF). As an example, the linear-elastic plane-strain fracture toughness K_{IC} of metallic materials can be determined, for instance, by using the specimen and loading conditions defined in the ASTM E399 standard [1], which isolates mode I (symmetric mode) at the crack tip neighbourhood.

The generalized stress intensity factors (GSIFs) have shown to control the onset of failure at sharp notches, see Reedy and Guess [2] in butt joints Dunn et al. [3] at sharp notches in PMMA, Qian and Akisanya [4] in bimaterial bonded joints, and Carpinteri et al. [5] in V-notches using also finite fracture mechanics. Characterization in mixed modes at bimaterial interfaces can be found in Dollhofer et al. [6].

In Part I, Barroso *et al.* [7], the explicit representation of the asymptotic stress field by means of a series expansion controlled by the GSIFs for any generic anisotropic multimaterial corner has been obtained. In the same paper, a procedure which allows the definition of a loading case to isolate any of the two singular terms of this stress representation has been developed, for the particular case of closed corners (with all material wedges bonded together), sometimes referred to as a cross point.

The proposed procedure is essentially focused on multimaterial closed corners having two stress singularities. Multimaterial corners having only one singularity present no significant difficulty in the determination of the critical value of the GSIF (denoted in what follows as Generalized-Fracture-Toughness) as it is only necessary to obtain the failure load and use it in the local stress field representation controlled by only one singular term. In the case of there being two singularities it is necessary to define the geometry and loading conditions to isolate either of them, which is not a straightforward task. The lack of symmetries in the stress fields in general configurations of anisotropic multimaterial corners makes it difficult to develop a general procedure for the determination of the Generalized-Fracture-Toughness in corners of this kind.

The procedure introduced in Part I, Barroso *et al.* [7], permits the definition of such test configurations for multimaterial closed corners and has no limitations either in the number or the nature of the materials (isotropic, orthotropic, etc.) involved in the corner.

The approach followed in the present work is based on a linear elastic behaviour, what is considered consistent with the properties of the materials involved and the purpose of the work: the onset of the failure.

The present paper describes the manufacturing, testing and postprocessing of the experimental data from a bimaterial CFRP-Adhesive corner which was extensively analyzed in Part I of this work, Barroso *et al.* [7]. The proposed procedure is based on a novel modified configuration of the well-known Brazilian test geometry (introduced almost simultaneously by Carneiro [8] and Akazawa [9]), with the multimaterial corner at the centre of the disk. The disk is loaded in compression along any diameter, the procedure obviously being valid only for closed corners.

The Brazilian disk specimen has been shown to be a suitable test for measurements of fracture toughness of interface cracks by Banks-Sills et al. [10,11].

Although the procedure has been applied, in the present paper, to a bimaterial joint, there is no additional impediment to use it in three- or multi-material corner configurations, provided that the stress representation involves only two singular terms. Examples of composite three-material corners having two stress singularities have been extensively reported in literature, see for example Barroso et al. [12] for the detailed analysis of the three-material corner as that depicted in Figure 1, corner b.

Section 2 presents the manufacturing of the samples, Section 3 the test carried out, and Section 4 presents the evaluation of a failure envelope based on the Generalized-Fracture-Toughness values obtained by the experiments.

2 Manufacturing of the samples

A scheme of the bimaterial system under study is depicted in Figure 1a, where R and t are, respectively, the radius and thickness of the Brazilian disk specimen. A scheme of the load configuration is shown in Figure 1b, where α defines the diametric compressive load orientation.

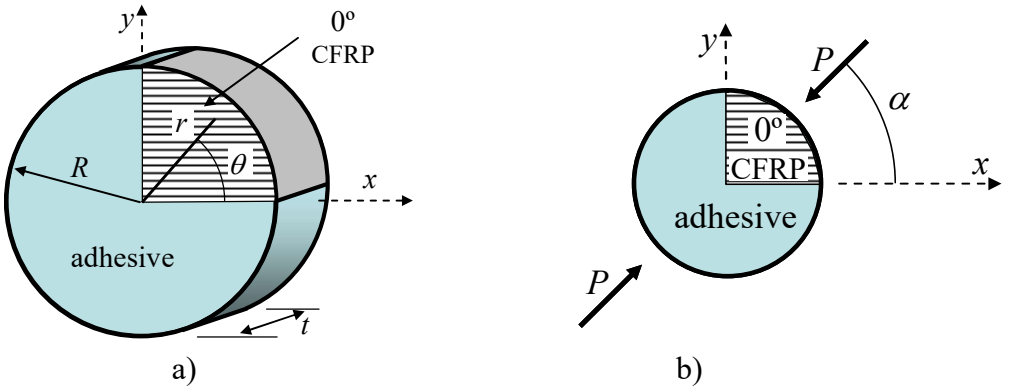

Figure 1. a) Geometry of a sample of the bimaterial CFRP-adhesive corner, b) scheme of the specimen loading.

The manufacturing of the samples for the uniaxial compression test was carried out using a vacuum bag and autoclave process. For the CFRP wedge, a carbon-epoxy laminate produced by curing 150 unidirectional plies was used. The manufacturing process can be schematically divided into the following steps, schematized in Figure 2.

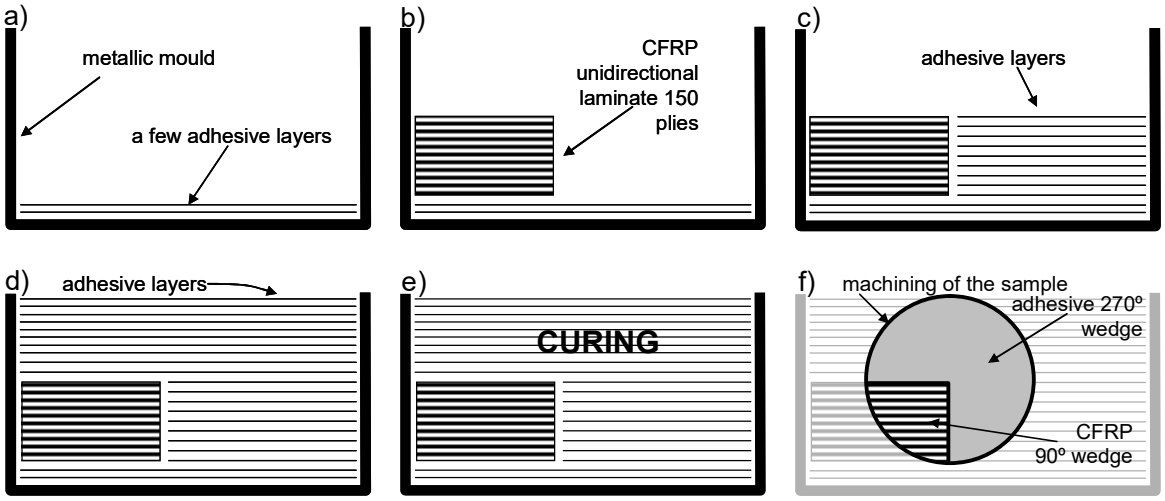

Figure 2. Scheme of the sample fabrication, a) adhesive layer in the mould, b) cured 150-ply CFRP laminate, c) adhesive layers to complete laminate thickness, d) additional adhesive layers, e) autoclave curing, f) machining of the Brazilian disk sample.

A few layers of adhesive were placed over the mould, Figure 2a, in order to cover the possible irregularities of the mould surface and to promote a good adhesion between the carbon laminate (wrapped in adhesive) and the other adhesive layers. Previously, the mould was covered with a Teflon layer to make the demoulding step easier at the end of the curing process.

The composite laminate (150 plies of a unidirectional CFRP) wrapped in an adhesive layer to assure a proper adhesion between the two materials, was placed over the adhesive layers, at one lateral side of the mould, Figure 2b.

Then adhesive layers were placed over the laminate and the mould, see Figures 2c and 2d. The compaction of the plies was carried out using a Teflon spatula and, after the compaction of 4 adhesive plies, an intermediate vacuum bag was prepared to improve compaction and bonding. Once the whole part was compacted, a lay-up of cork layers was placed at the sides of the joint to prevent the escape of adhesive during the curing cycle.

After the lay-up and compaction process, the system was prepared for autoclave curing, Figure 2e. A vacuum bag was constructed over the mould to ensure compaction during the curing process and to avoid the contact of the adhesive with the air (which would produce a bad curing state).

For the vacuum bag, a Teflon film was first placed, to help the demoulding of the part once cured. After that, an air breather fabric (Airweave®) was placed to make the vacuum uniformly distributed throughout the mould. Finally, a vacuum bag plastic layer was placed to cover the bag and was sealed with a sealant tape. Two vacuum valves were placed inside the bag to make and to measure the vacuum during the process, respectively. The curing cycle for the adhesive was 60 minutes at 120ºC and 0.28 MPa (with a heating ramp of 30 minutes, from room temperature to 120ºC).

After curing, the system was demoulded and visually inspected to check that the process (both the curing and the compaction) had been carried out properly. To prepare the samples, the bimaterial system was cut with a water-cooled diamond disk saw to a thickness of $7^{\pm 1}$ mm and a radius of $17^{\pm 1.5}$ mm. The exact dimensions of each specimen will obviously be taken into account in the evaluation of the Generalized-Fracture-Toughness. Then the samples were suitably marked and machined to obtain the circular specimens for the uniaxial tests, Figure 2f.

Some pictures of the real manufacturing process are shown in Figure 3.

a) 

b) 

c) 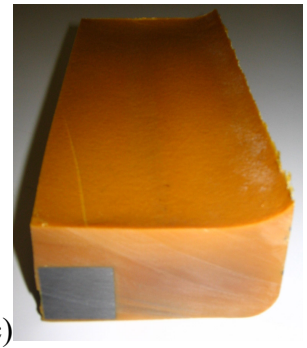

d) 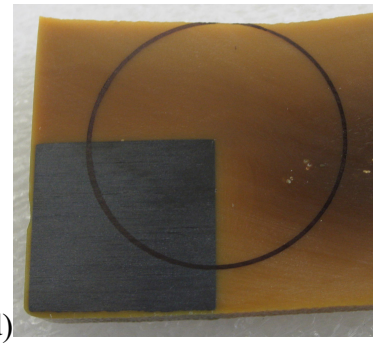

e) 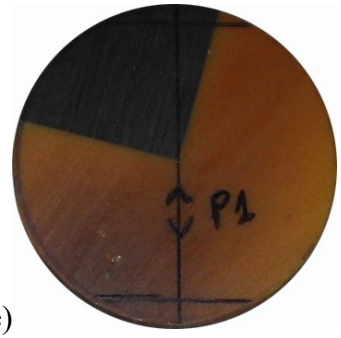

Figure 3. a) Lamination of adhesive layers, b) vacuum bag, c) sample after curing, d) slice, e) final circular sample

Figure 3a shows the bimaterial system (adhesive-CFRP) completely laminated previous to the preparation of the vacuum bag, shown in Figure 3b. After the autoclave curing, the cured block is shown in Figure 3c. Slices of the block, Figure 3d, are cut using a water-cooled diamond disk, and the final circular shape, Figure 3e, is obtained from these slices.

3. Uniaxial tests of the samples

The samples were suitably prepared for the application of the compression load, which should be distributed along a small flat area at both sides, as is usually recommended in the standard Brazilian test to avoid premature failure (Wang and Xing [13]). The samples were tested in compression as shown in Figure 4a. Figure 4b shows a detail of the sample after failure.

The numerical analysis performed in Part I of this work (Barroso *et al.* [7]) defined the angles α (Figure 1b) at which the compression of the samples would produce a pure singular term at the corner tip neighbourhood. These angles were determined at approximately $\alpha \approx 13^{\circ}$ and $\alpha \approx 60^{\circ}$.

These two testing orientations will enable the Generalized-Fracture-Toughness K_{1C} and K_{2C} to be evalued. Then the testing at other angles will permit the evaluation of a failure envelope based on GSIF values at the corner tip. Table 1 shows, for each specimen, thickness, radius and failure load. Figure 5 shows a sample of the cracked specimens and a schematic representation of the failure path for some of the chosen load orientations $0^{\circ}<\alpha<90^{\circ}$ including those where K_2 and K_1 vanish, $\alpha \approx 13^{\circ}$ and $\alpha \approx 60^{\circ}$ respectively. In particular, Figure 5 shows the cases of $\alpha=0^{\circ}$, $\alpha=13^{\circ}$, $\alpha=30^{\circ}$, $\alpha=60^{\circ}$ and $\alpha=90^{\circ}$, respectively.

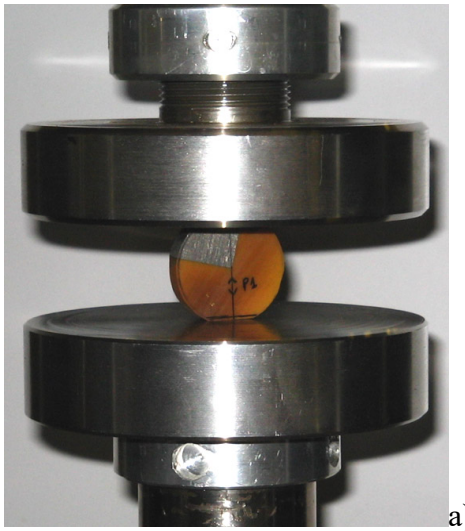
a)

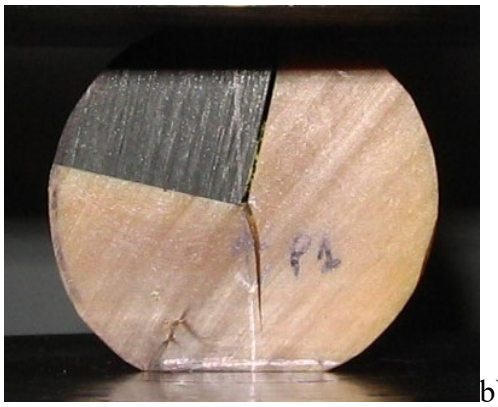
b)

Figure 4. a) Compression plates with a sample before failure, b) detail of the sample with α=13º after failure.

Load angle (α)	sample	thickness (mm)	radius (mm)	failure load (N)
0º, 180º	a	7.50	16.94	10212
	b	7.36	15.06	7675
	c	6.20	15.67	7272
	d	6.66	17.74	8275
13º (K_2≈0)	a	7.22	15.67	8952
	b	8.20	15.80	12449
	c	7.64	17.21	10565
30º	a	7.50	15.00	8625
	b	7.58	18.12	9859
	c	7.64	17.94	9607
60º (K_1≈0)	a	7.34	15.20	8667
	b	7.65	17.95	11998
	c	7.70	18.03	12782
90º	a	7.24	15.85	7624
	b	7.69	16.68	9188
	c	6.74	15.80	8295
	d	6.40	17.47	7627
115º (K_2≈0)	a	7.36	15.93	9346
	b	6.60	17.50	9898
	c	5.80	18.50	9033
120º	a	6.68	17.25	10879
	b	6.23	18.19	10104
143º (K_1≈0)	a	7.45	15.78	8153
	b	6.75	18.18	11252
	c	6.65	16.81	7360
150º	a	6.12	18.22	7209

Table 1. Results of the experimental tests.

α=0º

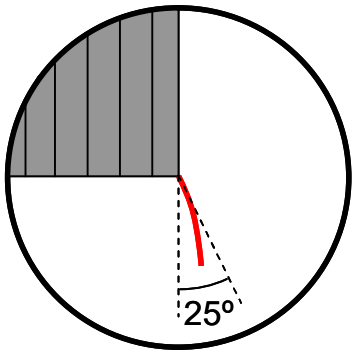

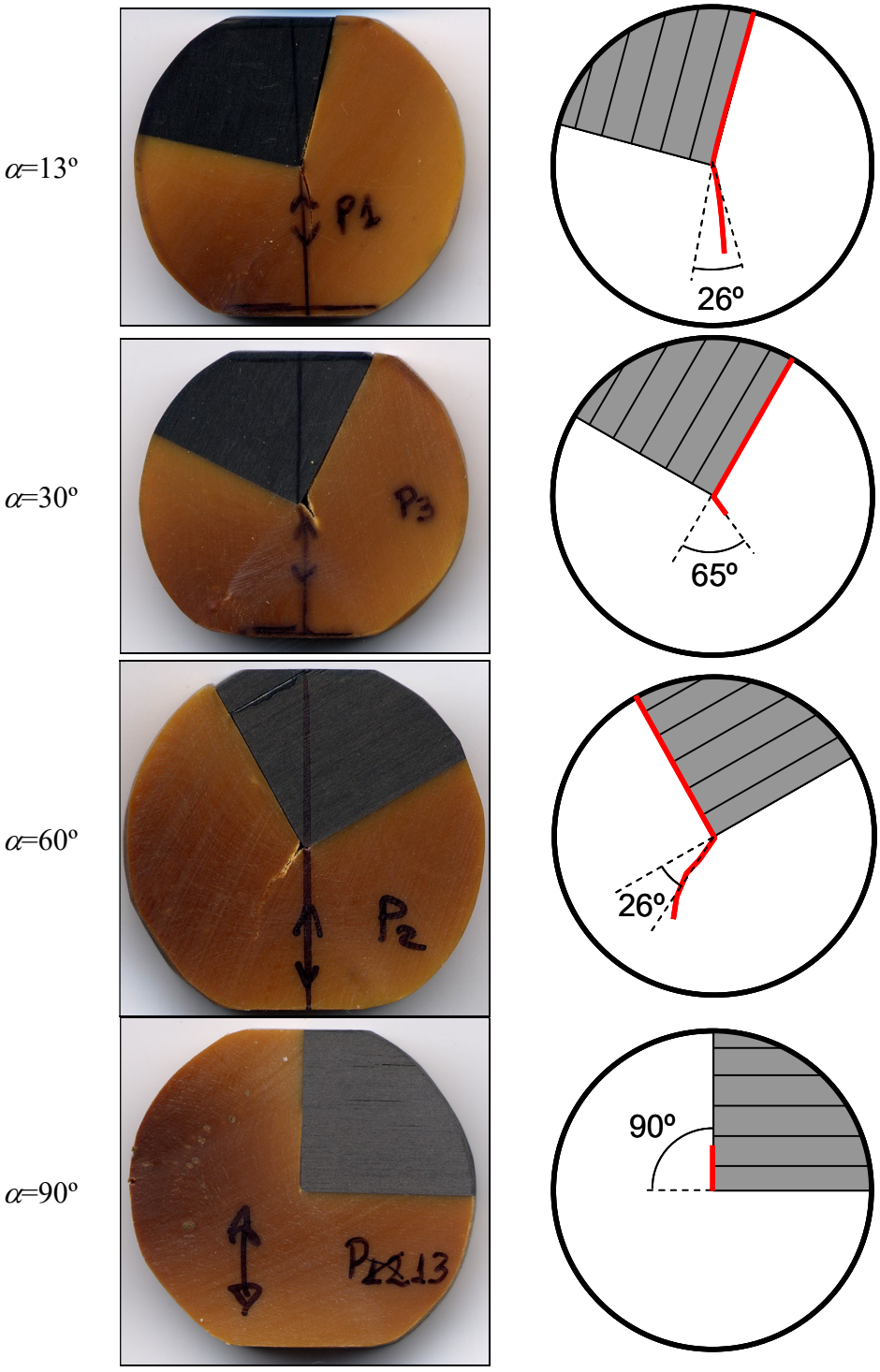

Figure 5. Tested samples and failure schemes (α=0º, 13º, 30º, 60º and 90º).

4. Generalized-Fracture-Toughness and failure envelope

To evaluate the critical value of the GSIFs in experiments from the previous numerical calculations by FEM, the experimental results have to be properly scaled with the data from the real tested specimens, summarized in Table 1. In particular, the critical value of the GSIFs can be obtained by means of the following expression:

$$K_{kC} = K_k^{FEM} \frac{t^{FEM}}{t^{\exp}} \frac{R^{FEM}}{R^{\exp}} \frac{P^{\exp}}{P^{FEM}} \left(\frac{R^{\exp}}{R^{FEM}} \right)^{1-\lambda_k} = K_k^{FEM} \frac{\sigma_{nom}^{\exp}}{\sigma_{nom}^{FEM}} \left(\frac{R^{\exp}}{R^{FEM}} \right)^{1-\lambda_k} \quad (1)$$

where superscripts "FEM" and "exp" denote values in the FEM analysis and experimental tests, respectively. $P^{\exp}$ is the experimental failure load (in N), $t^{\exp}$ is the real specimen thickness (in mm) and $R^{\exp}$ is the real specimen radius (in mm). The following values: P^{FEM}=100 N, t^{FEM}=1 mm, R^{FEM}=1 mm were used in the numerical model in [7]. Finally, $\sigma_{nom}^{\exp}$ and σ_{nom}^{FEM} are some nominal stresses in the numerical model and experimental specimen, respectively.

The presence of the FEM/exp ratios for P, t and R in (1) are simple relations derived from the dimensional analysis of a linear elastic problem, see equation (2) in [7]. Stresses in plane strain states are proportional to the value of the force per unit thickness (P/t) and the associate GSIFs are proportional to the stresses, this proportionality explicitly appearing in (1). It is also well known that stresses in a plane problem, with loads in terms of forces, are inversely proportional to the size-scale of the problem. In particular, the nominal stress state at the centre of the disk in the standard Brazilian Test configuration is inversely proportional to the radius R, e.g. see [8], and this inverse proportionality also explicitly appears in (1).

As the paper deals exclusively with failure onset, the criterion for determining $P^{\exp}$ was the value of the maximum load just before a sudden load decrement (in those specimens showing a brittle failure) or the value of the load when a visible damage (no magnification used) was observed followed by a progressive load decrement (for those specimens showing a more ductile failure).

In (1), the influence of the interface is implicitly taken into consideration in the procedure itself. Thus, corners with different properties of the interface may have different values of the generalized fracture toughness properties, if the interface is involved in the failure.

For the α=13º case, the following normalized values, according to Pageau *et al*. [14], were obtained: K_1 = 0.01125 MPa·mm$^{0.2367}$, K_2 = 0.007319 MPa·mm$^{0.1106}$, while for the α=60º case, the computed values were: K_1 = -0.0003594 MPa·mm$^{0.2367}$, K_2 = -0.1158 MPa·mm$^{0.1106}$. Using equation (1) the Generalized-Fracture-Toughness values K_{1C} and K_{2C} can be calculated, see Table 2, where individual values of the three samples have been included together with the mean value, standard deviation and variation coefficient (VC in %). All the singular parameters of the problem (order of singularities and generalized stress intensity factors, among others) were obtained using procedures developed by the authors [15,16].

	sample					
	a	b	c	mean value	standard deviation	VC (%)
K_{1C} (α=13º) (MPa·mm$^{0.2367}$)	0.017077	0.020778	0.017731	0.018529	0.001975	10.7
K_{2C} (α=60º) (MPa·mm$^{0.1106}$)	-0.121536	-0.139235	-0.146788	-0.135853	0.012961	9.5

Table 2. Generalized-Fracture-Toughness values K_{1C} and K_{2C}.

Due to the fact that K_{1C} and K_{2C} have different units (because of the different values of the orders of stress singularities associated to each of the terms), it is advisable to divide the critical values of K_k for other load orientations by the mean value of K_{kC} in order to eliminate these units. This will enable a simple graphical planar representation of all these critical values for all load orientations tested to be obtained. In this sense, figure 6 shows the dimensionless values of critical values of K_k obtained in all experiments.

The curve plotted in figure 6 represents an approximation of the failure envelope proposed by equation (3) in [7], the interior part of the envelope corresponding to the safe zone. In figure 6, ψ and $\kappa_C(\psi)$, defined in [7], represent a normalized fracture-mode-mixity angle and the critical normalized GSIF modulus, respectively. Recall that the failure envelope is independent of the size of the specimen.

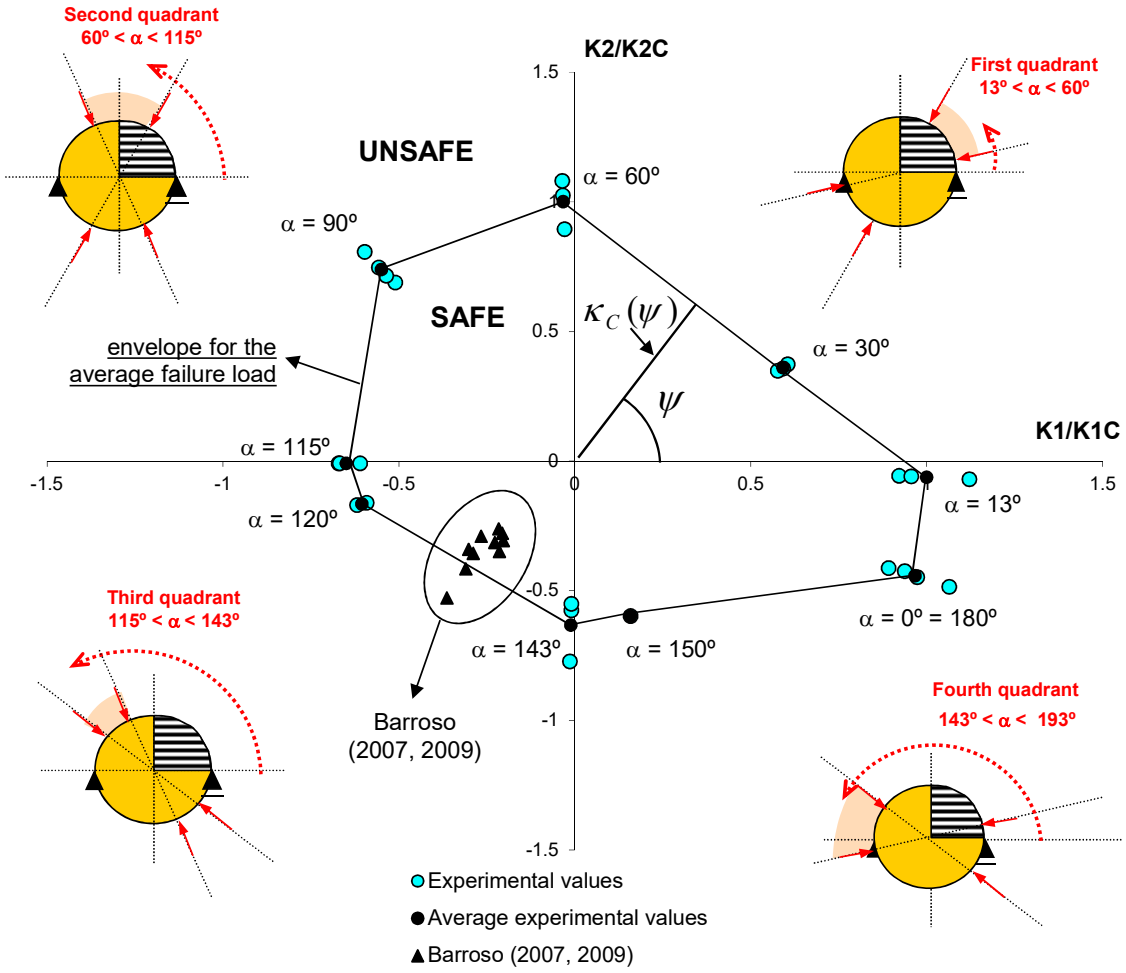

Figure 6. Failure envelope based on Generalized-Fracture-Toughness values of the corner.

Hafiz et al. [17] obtained for a different adhesively bonded joint system a similar failure envelope, but based on the strain energy release rate instead of GSIFs.

Each quadrant of the representation in Figure 6 is associated to particular loading angles of the modified Brazilian Test proposed here, information which has also been included in the figure. If the procedure proposed in Barroso et al [7] would not give load configurations in which K_1=0 or K_2=0, e.g. see figure 3a in [7], the experimental data would fall at the failure envelope part inside one quadrant. Recall that the complete failure envelope is a closed curve around the origin of the K_1-K_2 plane.

It can be observed in Figure 6 that the repeatability of the results for each load orientation is satisfactory, with a low dispersion of results.

Each set of experimental results, associated to the same load orientation angle α, falls along the same radial line in Figure 6, due to the fact that the ratio between (K_1/K_{1C}) and (K_2/K_{2C}) is constant for a constant value of α, the only difference being the value of the failure load. The failure envelope has been defined using the mean values of critical GSIFs K_k for each loading angle, and linear interpolation between loading angles.

Additionally, experimental results by Barroso [18,19], testing adhesively bonded double-lap joints with the same local geometry at the end of the overlap zone, in the joint of the unidirectional laminate corner with the adhesive spew fillet, have been included in Figure 6.

The results by Barroso [18,19] correspond to complete failure of the double-lap joints under consideration, while the present results correspond in all cases to failure initiation, as can be observed in some of the broken samples in Figure 5, where the failure path did not reach the outer boundaries. These results fall very close to the failure envelope obtained in the present work. This result is quite significant as the samples tested in Barroso [18,19], although they have the same local corner configuration, are completely different in size, geometry and manufacturing process. While the Brazilian disk specimens have been manufactured in autoclave and have a characteristic distance from the corner of 17 mm (the diameter), the double-lap joints have been manufactured in a hot plate press and have a characteristic distance of 0.1 mm (the adhesive thickness).

It is clear from results in Figure 6 obtained in [18,19] that double-lap joints subjected to shear by a tensile load fall inside the third quadrant. A deeper analysis of the failure criterion of such specimens based on critical values of the Generalized-Fracture-Toughness would imply a higher number of tests inside this third quadrant.

Load angle / sample		$\frac{K_1}{K_{1C}}$	$\frac{K_2}{K_{2C}}$
0º, 180º	a	1.06	-0.49
	b	0.89	-0.41
	c	0.97	-0.45
	d	0.94	-0.43
13º (K_2≈0)	a	0.92	-0.06
	b	1.12	-0.07
	c	0.96	-0.06
30º	a	0.60	0.37

Load angle / sample		$\frac{K_1}{K_{1C}}$	$\frac{K_2}{K_{2C}}$
90º	a	-0.51	0.69
	b	-0.56	0.75
	c	-0.60	0.81
	d	-0.54	0.71
115º (K_2≈0)	a	-0.61	-0.01
	b	-0.67	-0.01
	c	-0.67	-0.01
120º	a	-0.62	-0.17

	b	0.59	0.36
	c	0.58	0.35
60º (K_1≈0)	a	-0.03	0.89
	b	-0.03	1.02
	c	-0.04	1.08

	b	-0.59	-0.16
143º (K_1≈0)	a	-0.01	-0.58
	b	-0.01	-0.77
	c	-0.01	-0.55
150º	a	0.16	-0.60

Table 3. Results of K_1/K_{1C} and K_2/K_{2C}.

In [7], it was observed that there were other load orientations, α≈143º for K_1 and α≈115º for K_2, at which the corresponding singular term also vanished. Choosing these load orientations instead of α≈13º and α≈60º, to define K_{1C} and K_{2C} would not a relevant influence on the failure envelope shape (Figure 6 of the present paper). It would only affect the scale of the failure envelope, as results in Table 3 would have unit values, for K_1/K_{1C} and K_2/K_{2C} at α≈115º and α≈143º respectively.

5. Conclusions

In the present work an experimental test procedure has been developed for Generalized-Fracture-Toughness determination in multimaterial closed corners. The procedure is based on a novel modified configuration of the well-known Brazilian test applied to corner geometry, as a result of which the procedure is only valid for closed corners that can be loaded in compression in the diametric direction at any point along the whole external perimeter.

The procedure is especially suitable for non-symmetric multimaterial corners involving isotropic and non-isotropic materials and having two stress singularities. The procedure is able to isolate any of the singular modes, which is not possible with standard test procedures defined for homogeneous isotropic materials, due to the lack of general symmetries of the local stress states at these corners.

The procedure has been applied to a particular bimaterial corner typically appearing in adhesive joints involving composites and Generalized-Fracture-Toughness values K_{1C} and K_{2C} have been obtained. With the Generalized-Fracture-Toughness values, a failure envelope based on the GSIF values has been defined, which can be used as a failure criterion in joints of this type.

Previous experimental results already published, involving the same local corner configuration but completely different global geometry, have proved to be in good agreement with the proposed failure envelope.

The present procedure can be extended to other multimaterial systems with different local corner configurations, including two or more materials, provided they have only two stress singularities at all, or at the most two in-plane stress singularities which can be uncoupled from the antiplane one. The procedure would require carrying out the pertinent experiments and numerical calculations similar to those developed herein.

6. Acknowledgements

This work was supported by Junta de Andalucía and European Social Fund through the Projects of Excellence P08-TEP-4071 and P08-TEP-4051, by Ministerio de Ciencia e Innovación through project MAT2009-14022 and also by CAPES Brazilian Ministry of Education for a Doctoral Fellowship for Ms. Daniane Vicentini.

7. References

[1] ASTM Standard E399 - 2009e2, "Standard Test Method for Linear-Elastic Plane-Strain Fracture Toughness KIc of Metallic Materials", ASTM International, West Conshohocken, PA, 2003, DOI: 10.1520/E0399-09E02, www.astm.org.
[2] Reedy ED and Guess TR. Comparison of butt tensile strength data with interface corner stress intensity factor prediction. Int J Solids Struct 1993; 30: 2929-2936.
[3] Dunn ML, Suwito W and Cunningham S. Fracture initiation at sharp notches: correlation using critical stress intensities. Int. J. Solids Struct 1997; 34: 3873-3883.
[4] Qian Z and Akisanya AR. An experimental investigation of failure initiation in bonded joints. Acta Mater. 1988; 46: 4895-4904.
[5] Carpinteri A, Cornetti P, Pugno N, Sapora A and Taylor D. A finite fracture mechanics approach to structures with sharp V-notches. Eng Fract Mech 2008; 75: 1736-1752.
[6] Dollhofer J, Beckert W, Lauke B and Schneider K. Fracture mechanical characterization of mixed-mode toughness of thermoplast/glass interfaces. Com Mater Sci 2000; 19: 223-228.
[7] Barroso A, Vicentini D, Mantič V and París F. Determination of generalized fracture toughness in multimaterial closed corners with two singular terms. Part I: procedure and numerical results. Eng Fract Mech (submitted for publication) 2011.
[8] Carneiro FLLB. A new method to determine the tensile strength of concrete. In: Proceedings of the 5th meeting of the Brazilian Association for Technical Rules 1943 126-129.
[9] Akazawa T. Méthode pour l'essai de traction de bétons. Journal of the Japanese Civil Engineering Institute 1943. Republished in French by the Bulletin RILEM 16 Paris 1953: 13-23.
[10] Banks-Sills L, Konovalov N and Fliesher A. Comparison of two- and three-dimensional analyses of interface fracture data obtained from Brazilian disk specimens. Int J Struct Integrity 2010; 1:20-42.
[11] Banks-Sills L, Travitzky N, Ashkenazi D and Eliasi R. A methodology for measuring interface fracture toughness of composite materials. Int J Fracture 1999; 99: 143–161.
[12] Barroso A, Mantič V and París F. Computing stress singularities in transversely isotropic material corners by menas of explicit expressions of the orthonormalized Stroh-eigenvectors. Eng Fract Mech 2009c; 76: 250-268.
[13] Wang QZ and Xing L. Determination of fracture toughness K_{IC} by using the flattened Brazilian disk specimen for rocks. Engi Fract Mech 1999; 64: 193-201.
[14] Pageau SP, Gadi KS, Biggers Jr. SB and Joseph PF. Standardized complex and logarithmic eigensolutions for n-material wedges and junctions. Int J Fracture 1996; 77: 51-76.
[15] Barroso A, Mantič V and París F. Singularity analysis of anisotropic multimaterial corners. Int J Fracture 2003; 119: 1-23.

[16] Barroso A, Graciani E, Mantič V and París F. A least squares procedure for the evaluation of multiple generalized stress intensity factors at 2D multimaterial corners by BEM. Eng Anal Bound Elem (in press) 2011.
[17] Hafiz TA, Abdel Wahab MM, Crocombe AD and Smith PA. Mixed-mode fracture of adhesively bonded metallic joints under quasi-static loading. Eng Fract Mech 2010; 77: 3434-3445.
[18] Barroso A. Characterization of singular stress fields in multimaterial corners. Application to adhesive joints with composite materials. Ph.D. Thesis (in Spanish), University of Seville 2007.
[19] Barroso A, París F and Mantič V. Representativity of the singular stress state in the failure of adhesively bonded joints between metals and composites. Compos Sci Techol 2009; 69: 1746-1755.